British Journal of Pharmacology (2008) 155, 945–956

0007–1188/08 $32.00
www.brjpharmacol.org

RESEARCH PAPER

The antioxidant activity of chondroitin-4-sulphate, in carbon tetrachloride-induced acute hepatitis in mice, involves NF-κB and caspase activation

GM Campo, A Avenoso, S Campo, G Nastasi, P Traina, A D'Ascola, CA Rugolo and A Calatroni

Department of Biochemical, Physiological and Nutritional Sciences, Section of Medical Chemistry, School of Medicine, University of Messina, Policlinico Universitario, Messina, Italy

Background and purpose: Reactive oxygen species (ROC) are the main causes of carbon tetrachloride (CCl_4)-induced acute liver injury. Chondroitin-4-sulphate (C4S) is known to inhibit lipid peroxidation through antioxidant mechanisms. Activation of nuclear factor (NF)-κB and caspases may strongly intensify inflammation and cell damage, in addition to that directly exerted by ROS. We investigated whether treatment with C4S, besides exerting antioxidant activity, was able to modulate NF-κB and apoptosis activation in CCl_4-induced liver injury in mice.
Experimental approach: Acute hepatitis was induced in mice by an i.p. injection of CCl_4. Varying doses of C4S were administered i.p. 1 h before, 6 and 12 h after CCl_4 injection. 24 h after CCl_4 injection, the mice were killed for biochemical and histological analysis.
Key results: CCl_4 injection produced: marked elevation of alanine aminotransferase and aspartate aminotransferase; hepatic membrane lipid peroxidation, assayed by 8-isoprostane levels; and depletion of reduced glutathione and superoxide dismutase. CCl_4 also decreased NF-κB translocation and IkBα, and increased gene expression of mRNA and protein of metalloproteases (MMP)-2 and -9, and of pro- and cleaved forms of caspases-3 and -7. There was also increased liver polymorphonuclear infiltration, evaluated by elastase assay, and hepatic cell disruption.
C4S treatment inhibited lipid peroxidation; blocked NF-κB activation and IkBα protein loss; decreased mRNA and proteins for MMPs and caspases; restored endogenous antioxidants; limited hepatic polymorphonuclear accumulation and tissue damage.
Conclusions and implications: As antioxidants may inhibit NF-κB and caspase activation, we hypothesize that treatment with C4S was able to inhibit NF-κB and apoptosis activation in hepatic injury.
British Journal of Pharmacology (2008) **155,** 945–956; doi:10.1038/bjp.2008.338; published online 25 August 2008

Keywords: antioxidants; caspases; carbon tetrachloride; liver damage; chondroitin-4-sulphate; NF-κB; oxidative stress; free radicals

Abbreviations: ALT, alanine aminotransferase; AST, aspartate aminotransferase; C4S, chondroitin-4-sulphate; CS, chondroitin sulphate; ECM, extracellular matrix; ELA, elastase; GSH, reduced glutathione; 8-IPE, 8-isoprostane; MMP, metalloprotease; NF-κB, nuclear factor-κB; PBS, phosphate-buffered saline; ROS, reactive oxygen species; SOD, superoxide dismutase

Introduction

It is known that acute and chronic hepatic injury, which cause high morbidity and mortality world-wide, are induced by a disparate range of pathophysiological conditions. Liver intoxication has increased as a result of exposure to high levels of environmental toxins (Pineiro-Carrero and Pineiro, 2004). This is because the liver has an important role in detoxification (Wang *et al.*, 2007). Although the pathogenesis of acute cirrhosis is not fully understood, it is clear that reactive oxygen species (ROS) have a key function in pathological changes in the liver (Stehbens, 2003; Wu *et al.*, 2006). In fact, studies of causative factors involving liver injury have been performed for a number of years now, and it is well known that ROS are heavily involved in the cause and progression of hepatic damage (Stehbens, 2003; Wu *et al.*, 2006). Biological membranes are particularly susceptible to ROS effects. The peroxidation of unsaturated fatty acids in biological membranes produces: first a decrease in fluidity, then loss of function, disruption of integrity and finally, cell death (Stehbens, 2003; Wu *et al.*, 2006). Carbon

Correspondence: Professor GM Campo, Department of Biochemical, Physiological and Nutritional Sciences, School of Medicine, University of Messina, Policlinico Universitario, Torre Biologica, 5° piano, Via C. Valeria 98125, Messina, Italy.
E-mail: gcampo@unime.it
Received 10 July 2008; revised 17 July 2008; accepted 22 July 2008; published online 25 August 2008

tetrachloride (CCl_4), a hepatotoxin, has been used extensively to induce liver injury in various animal models for decades (Weber *et al*., 2003). The experimentally induced cirrhotic response by CCl_4 in rats and mice has been shown to be similar to human cirrhosis of the liver (Weiler-Normann *et al*., 2007).

Even though the relationship between oxidative stress, cytotoxic cytokines and liver cell injury has not been fully clarified, nuclear factor (NF)-κB is believed to have a pivotal function at this stage (Heyninck *et al*., 2003). NF-κB plays an essential and beneficial role in normal physiology; however, the upregulation of this factor has been implicated in the pathogenesis of several diseases, including inflammation and liver diseases (Heyninck *et al*., 2003). Animal models of acute hepatic damage also support the idea that NF-κB has a very active function in the development and progression of cirrhosis (Heyninck *et al*., 2003). NF-κB signalling pathways mediate critical events in the inflammatory response through hepatocytes, which lead to progressive extracellular matrix (ECM) damage and cell destruction. Activation of stellate cell (lipocytes) is a critical stage in liver damage, but the mechanisms leading to stellate cell activation *in vivo* are not completely understood. The characteristic hepatic oxidative stress cascade induced *in vivo* by CCl_4 markedly stimulated stellate cell entry into S phase, NF-κB activity and c-myb expression (Lee *et al*., 1997; Orfila *et al*., 2005). The synthesis of ROS, in fact, subsequently activates NF-κB, which has been known to contribute to vicious cycles of inflammatory reactions (Pantano *et al*., 2006). Overactivation of the fine-tuned apoptotic process can lead to significant hepatocellular damage. ROS may also have a significant function in promoting apoptosis (Malhi *et al*., 2006). It has been reported that molecules capable of scavenging ROS may reduce NF-κB and apoptosis activation in several types of liver disease (Sun *et al*., 2001; Waris *et al*., 2002; Ding and Yin, 2004).

Although oxidants are commonly considered to exert their effects through direct toxic action on target cells, recent findings suggest their contributory role in gene induction. NF-κB may be activated by low levels of ROS and inhibited by antioxidants (Bhattacharyya *et al*., 2004; Kundu *et al*., 2006).

The priming of apoptosis in hepatic tissue may contribute to liver damage and impaired function. During this process, caspases are activated through a protease cascade, whereby the inactive proenzyme is cleaved to form subunits of the active heterotetrameric protease (Schattenberg *et al*., 2006). Several distinctive cellular changes occur in apoptosis, including nuclear changes, such as chromatin condensation, internucleosomal DNA degradation, and nuclear lobulation and fragmentation. Other characteristics of the degradative phase of apoptosis are membrane blebbing, mitochondrial dysfunction, cellular and cytoplasmic shrinkage and endonuclease activation and finally, disintegration into small vesicles called apoptotic bodies (Malhi *et al*., 2006). A great deal of evidence indicates that cell exposure to ROS, in addition to producing direct chemical injury to cell components, also induces apoptosis, which leads to cell disruption and tissue necrosis (Ozben, 2007). Recent studies have reported that apoptosis stimulated by oxidative stress may be inhibited by a number of antioxidant molecules (Genestra, 2007).

Most biological molecules have more than one function. In particular, many molecules have the ability to directly/indirectly scavenge free radicals and thus act as antioxidants in living organisms. The increased levels of these molecules during oxidative stress seems to be a biological response that may protect cells from oxidation, in synergy with other antioxidant defence systems. One of these structures is the glycosaminoglycan, chondroitin-4-sulphate (C4S), a biomolecule that has increasingly focused the interest of many research groups because of its antioxidant activity (Campo *et al*., 2004c, 2006). Chondroitin sulphate (CS) is a complex glycosaminoglycan extracted and purified from various tissues. It is a ubiquitous component of all connective tissue ECM, where it serves a number of functions, mainly covalently attached to proteins in the form of proteoglycans. CS consists of alternating disaccharide units of glucuronic acid and galactosamine and is attached to serine residues of the protein cores through a tetrasaccharide linkage (Volpi, 2006). CS structures may be distinguished by means of their sulphation. They may be sulphated at the C-4 position of galactosamine giving C4S or at the C-6 position of galactosamine giving C6S. Despite the simplicity of the backbone structure, the CS molecule is complex enough to carry biological information and thus affects many biological functions. In recent years, CS has become the focus of attention by virtue of the important role it plays in wound healing; promoting neurite outgrowth, axonal regeneration, cell adhesion, cell division and the modulatory role of growth factors (Volpi, 2006).

Starting from these findings, the aim of this study was to investigate whether the antioxidant property of C4S, previously evaluated in a CCl_4-induced acute damage and liver fibrosis in rats (Campo *et al*., 2004a, b), involves NF-κB and caspase regulation, using, this time, a model of CCl_4-induced acute cirrhosis in mice.

Materials and methods

Animals

The studies reported in this paper have been performed in accordance with the Helsinki declaration and guidelines for the Care and Use of Laboratory Animals. The health of the animals was monitored in accordance with Italian Veterinary Board guidelines. Male mice CD-1, 6–7 weeks old with a mean weight of 25–30 g, were used in our study. Mice, purchased from Harlan (Correzzana, Italy), were maintained under climate-controlled conditions with a 12-h light/dark cycle. The animals were fed standard rodent chow and water *ad libitum*. Mice were divided into the following groups: (1) Control ($n=18$); (2) C4S ($120\,mg\,kg^{-1}$) ($n=18$); (3) CCl_4 ($n=20$); (4) CCl_4 + C4S ($30\,mg\,kg^{-1}$) ($n=18$); (5) CCl_4 + C4S ($60\,mg\,kg^{-1}$) ($n=18$) and (6) CCl_4 + C4S ($120\,mg\,kg^{-1}$) ($n=18$). Additional groups of mice were used to establish whether C4S may affect bioactivation of CCl_4 or the rate of reduced glutathione (GSH) resynthesis.

Induction of acute toxic hepatitis

Mice were injected i.p. with CCl_4 (1.0 mL kg^{-1} body weight in a ratio of 1:1 (v/v)) in mineral oil solution and controls with the same dose of mineral oil. Animals were given food and water *ad libitum* throughout the experiment. Mice were killed under ether anaesthesia, 24 h after CCl_4 treatment, at which time blood was collected from the inferior vena cava and the livers were isolated. The collected blood was then separated into serum. The isolated livers were kept at 4 °C for histological and biochemical tests.

C4S treatment

On the day of the experiment, the mice were randomized to receive treatment with C4S at doses of 30, 60 and 120 mg kg^{-1}. The first C4S administration was carried out 1 h before CCl_4 injection, the second and the third were administered 6 and 12 h after CCl_4 treatment. C4S was dissolved in saline solution (0.9% NaCl) and administered i.p. (1.0 mL kg^{-1} body weight).

Serum alanine aminotransferase and aspartate aminotransferase measurement

Alanine aminotransferase (ALT) and aspartate aminotransferase (AST) were evaluated in serum samples (100 μL) obtained 24 h after CCl_4 treatment. Activities were assayed using the commercial clinical test kits (Roche Diagnostic, Milan, Italy).

NF-κB p50/65 transcription factor assay

Nuclear factor-κB p50/65 DNA-binding activity in nuclear extracts of hepatic tissue samples was evaluated to measure the degree of NF-κB activation. The assay combines the principle of the electrophoretic mobility shift assay with the ELISA. Analysis was performed in line with the manufacturer's protocol for a commercial kit (NF-κB p50/65 Transcription Factor Assay Colorimetric, cat. no. SGT510, Chemicon International Inc., Temecula, CA, USA). In brief, the livers of the animals were isolated at the end of the experimental phase, and maintained at 4 °C, washed in ice-cold (10 mM Tris-HCl, pH 7.4), and blotted on absorbent paper. Samples were then trypsinized and gently minced, using an automatic homogenizer (Ultra-Turrax, Wilmington, NC, USA), to isolate hepatic cells. Cytosolic and nuclear extraction was performed by lysing the cell membrane with a suitable hypotonic lysis buffer containing protease inhibitor cocktail and tributylphosphine as reducing agent. The lysate was then incubated on ice and centrifuged at $250 \times g$ for 15 min. Then after adding two volumes of buffer, a series of drawing and ejecting actions were then performed using a syringe with a small gauge needle. This step was carried out 5 times. After centrifugation at $8000 \times g$ for 20 min, the supernatant containing the cytosolic portion of cell lysate was recovered and stored at −70 °C for subsequent analysis. The pellet containing the nuclear portion was then resuspended in the extraction buffer and the nuclei were disrupted by a series of drawing and ejecting actions. After gentle stirring for 40 min, the nuclear suspension was centrifuged at $16\,000 \times g$ for 30 min. The supernatant fraction was the nuclear extract. After protein concentration was determined and adjusted to a final concentration (approximately 4.0 mg mL^{-1}), this extract was stored in aliquots at −80 °C for subsequent NF-κB assay. The analysis comprised a series of controlled steps accomplished by adding to the nuclear extract the following components: HeLa whole cell extract (tumour necrosis factor-α treated); transcription factor assay probe, NF-κB competitor oligonucleotide; NF-κB capture probe and enhanced transcription factor assay buffer to obtain the transcription factor assay as: normal, positive control, specific competitor control and negative control. After incubation with primary and secondary antibodies, colour development was then observed following the addition of the horseradish peroxidase substrate 3,3′, 5,5′tetramethylbenzidine. Lastly, the absorbance of the samples was measured at 450 nm, using a spectrophotometric microplate reader. Values are expressed as relative OD per mg of protein.

IkBα assay

IkBα loss was quantified in hepatic tissue samples to confirm NF-κB activation. The test is based on solid phase sandwich ELISA assay. The cytosolic fraction, obtained during the nuclei extraction procedure for NF-kB assay, was used for IkBα evaluation. The assay was carried out using a commercial kit (IkBα, Total BioAssay ELISA Kit, cat. no. 12500-05T, USBiological, Swampscott, MA, USA). Briefly, standards, samples and controls (0.1 mL) were added to each well of the coated microplate. After 2 h incubation at room temperature, the microplate was decanted and the liquid discarded. Wells were washed four times. Subsequently, anti-IkBα antibodies (0.1 mL) were added to each well. After 1 h incubation at room temperature, the liquid was again removed from the wells and these were washed 4 times, anti-rabbit IgG-horseradish peroxidase (0.1 mL) was added. After further incubation for 30 min and having washed the wells four times, stabilized chromogen (0.1 mL) was added. Absorbance was measured using a spectrophotometric microplate reader set at $\lambda = 450$ nm. Values are expressed as relative OD per mg of protein.

RNA isolation, cDNA synthesis and real-time quantitative PCR amplification

Total RNA was isolated from hepatic tissue for reverse-PCR real time analysis of metalloprotease (MMP)-2, MMP-9, caspase-3 and caspase-7 (RealTime PCR system, Mod. 7500, Applied Biosystems, Foster City, CA, USA). Total RNA was isolated from hepatic tissue using the Omnizol Reagent Kit (Euroclone, West York, UK). The first strand of cDNA was synthesized from total RNA (1.0 μg) using a high capacity cDNA Archive kit (Applied Biosystems). β-actin mRNA was used as an endogenous control to allow relative quantification of MMP-2, MMP-9 and caspase mRNAs (Bustin, 2000). Real-time PCR was performed by means of ready-to-use assays (Assays on demand, Applied Biosystems) on both targets and endogenous controls. The amplified PCR products were quantified by measuring the MMP-2, MMP-9, caspase and β-actin mRNA calculated cycle thresholds (C_t). The C_t values were plotted against log input RNA concentration in

serially diluted total RNA of hepatic tissue samples and used to generate standard curves for all the mRNAs analysed. The amounts of specific mRNA in samples were calculated from the standard curve and normalized with the β-actin mRNA. After normalization, the mean value of normal hepatic cell target levels became the calibrator (one per sample) and the results are expressed as the *n*-fold difference relative to normal controls (relative expression levels).

Western blot assay of MMP-2, MMP-9, procaspase-3, cleaved caspase-3, procaspase-7and cleaved caspase-7 proteins

For SDS-polyacrylamide gel electrophoresis and western blotting, the hepatic cells were washed twice in ice-cold phosphate-buffered saline (PBS) and subsequently dissolved in SDS sample buffer (62.5 mM. Tris-HCl, pH 6.8, 2% w/v SDS, 10% glycerol, 50 mM dithiothreitol, 0.01% w/v bromophenol blue). β-Actin protein was used as an endogenous control to allow the normalization of MMP-2, MMP-9, procaspase-3, cleaved caspase-3, procaspase-7 and cleaved caspase-7 proteins. Aliquots of whole cell protein extract (10–25 μL per well) were separated on a mini gel (10%). The proteins were blotted onto polyvinylidene difluoride membranes (Amersham Biosciences, Piscataway, NJ, USA) using a semidry apparatus (Bio-Rad Lab., Richmond, CA, USA). The blots were flushed with double-distilled H_2O, dipped into methanol and dried for 20 min before proceeding to the next steps. The blots were transferred to a blocking buffer solution (1 × PBS, 0.1% Tween 20, 5% w/v non-fat-dried milk) and incubated for 1 h. The membranes were then incubated with the specific diluted primary antibody in 5% BSA, 1 × PBS, and 0.1% Tween 20 in a roller bottle at 4 °C overnight. After being washed in three stages in wash buffer (1 × PBS, 0.1% Tween 20), the blots were incubated with the secondary polyclonal antibody goat anti-rabbit conjugated with peroxidase, in tris-buffered sodium/Tween-20 buffer, containing 5% non-fat-dried milk. After 45 min of gentle shaking, the blots were washed five times in wash buffer, and the proteins were made visible using an UV/visible transilluminator (EuroClone, Milan, Italy) and Kodak BioMax MR films. A densitometric analysis was also run to quantify each band.

Lipid peroxidation evaluation

Determination of 8-isoprostane (8-IPE) in the liver was carried out to evaluate the extent of oxidation of hepatic cell phospholipids by oxygen radicals. Analysis was performed using an EIA commercial kit (8-Isoprostane EIA kit, cat. no. 516351; Cayman Chemical Company, Ann Arbor, MI, USA). Briefly, the livers were removed at the end of the experimental phase and maintained at 4 °C, washed in ice-cold phosphate buffer (0.1 M, pH 7.4), containing EDTA (1.0 mM) and indomethacin (10.0 μM) and blotted on absorbent paper. Each sample was then minced in ice-cold enzyme immunosorbent assay (EIA) buffer, containing butylated hydroxytoluene (5.0 mg mL^{-1}) in ethanol and homogenized using an Ultra-Turrax homogenizer (1:10 (w/v) ratio at 4 °C). After centrifugation (5000 × *g* for 5 min at 4 °C), the supernatant was purified by affinity sorbent columns and the final eluent used for biochemical assay. Sample, 8-IPE AChE tracer and 8-IPE antiserum (50 μL) were added to each well. Then, the plate was covered with plastic film and incubated at room temperature for 18 h. After rinsing the wells five times with wash buffer, Ellman's reagent (0.2 mL) was added and the plate contents were gently mixed in the dark until colouration developed. Finally, the absorbance of each well was measured using a spectrophotometric microplate reader set at λ = 410 nm. A calibration curve of 8-IPE standard was also run for quantification. Values are expressed as relative OD per mg of protein.

GSH assessment

For GSH evaluation, hepatic tissue samples were homogenized using an Ultra-Turrax homogenizer (1:10 (w/v) ratio, at 4 °C), in a solution containing metaphosphoric acid (5%) acid and EDTA (5 mM). Each sample was then centrifuged (6000 × *g* at 4 °C for 10 min). The biochemical analysis was performed using a specific colorimetric assay (Bioxytech GSH-400 assay kit, cat. no. 21011, OxisResearch, Portland, OR, USA). Briefly, an aliquot (0.2 mL) of each supernatant was added in a polyethylene tube to potassium phosphate buffer (0.7 mL) containing diethylenetriamine pentaacetic acid and lubrol. After vortexing, 4-chloro-1-methyl-7-trifluoromethyl-quinolinum methylsulphate (50 μL) in HCl was added. The samples were vortexed again and NaOH (50 μL, 30%) was added. After vortexing, the samples were incubated at 25 °C in the dark for 10 min. The absorbance was then read at λ = 400 nm. The values of unknown samples were drawn from a standard curve plotted by assaying different known concentrations of GSH. The amount of hepatic GSH is expressed as nmol mg^{-1} of protein.

Superoxide dismutase determination

Superoxide dismutase (SOD) activity was determined in hepatic tissue samples after homogenization using an Ultra-Turrax homogenizer (1:10 (w/v) ratio, at 4 °C), in a solution of sucrose (0.25 M) containing diethylenetriamine pentaacetic acid (1.0 mM) and sonicated. After centrifugation (6000 × *g* for 20 min at 4 °C), the supernatant was collected and total SOD activity determined at 505 nm using a commercial kit (Ransod assay kit, Randox Laboratories, Crumlin, UK). In brief, diluted samples (50 μL, 1:10, v/v with 0.01 M potassium phosphate buffer, pH 7.0) were mixed with a solution (1.7 mL) containing xanthine (0.05 mM) and iodonitrotetrazolium chloride (0.025 mM). After mixing for 5 s, xanthine oxidase solution (0.25 mL, 80 U L^{-1}) was added. Initial absorbance was then read and the final absorbance was read after a further 3 min. SOD values are expressed as units per mg of protein.

Elastase evaluation

Elastase (ELA) activity was assayed to measure neutrophil accumulation and activation in hepatic tissue. The analysis was performed using a fluorometric commercial kit (Elastase Assay Kit, EnzChek, cat. no. E12056, Invitrogen, Eugene, OR, USA). Briefly, the livers were removed at the end of the experiment, washed in ice-cold Tris-HCl (10 mM, pH 7.4) and blotted on absorbent paper. Samples were then

homogenized, in the same washing buffer, using an Ultra-Turrax homogenizer (1:10 w/v) ratio. After centrifugation ($5000 \times g$ for 5 min at 4 °C), each supernatant (0.1 mL) was put into a tube containing diluted reaction buffer (0.45 mL) and fluorescently labelled elastine substrate (0.45 mL). After 2 h incubation, at room temperature covered to protect from light, fluorescence intensity was measured in a standard fluorometer at λ Ex 480 nm and λ Em 520 nm. A calibration curve of porcine pancreatic ELA standard was also run for quantification. Finally, a specific ELA inhibitor was used as control to eliminate any interference exerted by other proteases. Values are expressed as fluorescent arbitrary units (FAU) at λ Ex 480 nm and λ Em 520 nm mg^{-1} of protein.

Histological analysis

A histological examination was conducted to evaluate the degree of hepatic damage. The caudal portion from the liver of each mouse was removed at the end of the experimental phase and fixed by immersion in neutral-buffered formalin (10%). Fixed tissues were embedded in paraffin and cut into section (6.0 μm) (Blair *et al*., 1991). The sections were stained with haematoxylin–eosin and examined under light microscope (Optech Instrument, Munchen, Germany) connected to a digital camera (Coolpix 4500, Nikon, Japan).

Covalent binding of [^{14}C]-CCl_4 equivalents to liver proteins

To establish whether C4S had any effect on CCl_4 bioactivation-induced hepatic damage, the covalent binding of [^{14}C] equivalents of liver proteins was determined (Sawant *et al*., 2004). Briefly, [^{14}C]-CCl_4 (1.0 mL kg^{-1}, i.p., 32.0 μCi kg^{-1}) was administered in separate groups of mice with or without C4S. After 24 h, at the end of the experiment, mice were killed, livers excised and frozen in liquid nitrogen. Samples (2 g) of hepatic tissue were homogenized in 4.0 mL of ice-cold Tris-HCl buffer (pH 7.4), using an Ultra-Turrax homogenizer for 30 s at 4 °C. Two mL of homogenate was added to tubes containing 4.0 mL of ice-cold 100% ethanol, which precipitated proteins. The tubes were chilled in an ice bath for 15 min, vortexed and then centrifuged at $3000 \times g$ for 30 min. To remove lipids and non-covalently bound [^{14}C] equivalents, the pellets were extracted extensively with a series of washes with chloroform/methanol (3:1 v/v). The pellets (containing covalently bound [^{14}C]-CCl_4-derived radiolabel) were air-dried, dissolved in 1.0 mL of NaOH (1.0 M), and after the addition of 14.0 mL of liquid scintillation fluid (Ecolite +, MP Biomedicals, Seven Hills, Australia) the radioactivity was estimated by a liquid scintillation spectrometer (Beckman Coulter Inc., Fullerton, CA, USA). Values were expressed as disintegrations per minute per mg of tissue.

Protein analysis

The amount of protein was determined using the Bio-Rad protein assay system (Bio-Rad Lab.) with BSA as a standard in accordance with the published method (Bradford, 1976).

Statistical analysis

Data are expressed as means ± s.d. mean of no less than seven experiments for each test. All assays were repeated three times to ensure reproducibility. Statistical analysis was performed using one-way ANOVA followed by the Student–Newman–Keuls test. The statistical significance of differences was set at $P<0.05$.

Table 1 Effect of C4S treatment on serum AST and ALT levels in mice after CCl_4 injection

Experimental group	*AST*	*ALT*
Control (untreated)	34.5 ± 4.2	20.8 ± 3.2
C4S alone (120 mg kg^{-1})	31.2 ± 4.3	23.4 ± 3.4
CCl_4	187.7 ± 21.4†	158.2 ± 18.1†
CCl_4 + C4S (30 mg kg^{-1})	140.2 ± 17.4*	112.1 ± 15.5*
CCl_4 + C4S (60 mg kg^{-1})	110.4 ± 16.1*	88.3 ± 13.6*
CCl_4 + C4S (120 mg kg^{-1})	87.6 ± 13.2*	61.7 ± 12.4*

Abbreviations: ALT, alanine aminotransferase; AST, aspartate aminotransferase; CCl_4, carbon tetrachloride; C4S, chondroitin-4-sulphate.
Values are the mean ± s.d.mean of seven experiments and are expressed as U L^{-1}.
$^{\dagger}P<0.001$ vs control; $^{*}P<0.001$ vs CCl_4.

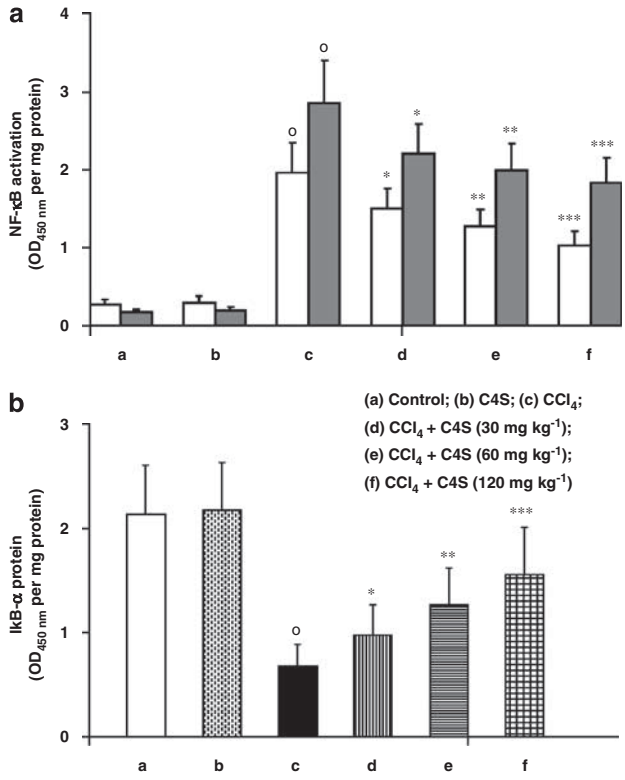

Figure 1 Effect of chondroitin-4-sulphate(C4S) treatment, with and without carbon tetrachloride (CCl_4) injection, on hepatic nuclear factor (NF)-κB p50/65 transcription factor DNA-binding activity (**a**) and IkBα protein degradation (**b**) in livers of mice. In panel **a**, data for both the p50 subunit and the p65 subunit of NF-κB are shown. The experimental conditions are indicated below each set of bars and in the key. (**a**) Control; (**b**) C4S (120 mg kg^{-1}); (**c**) CCl_4; (**d**) CCl_4 + C4S (30 mg kg^{-1}); (**e**) CCl_4 + C4S (60 mg kg^{-1}); (**f**) CCl_4 + C4S (120 mg kg^{-1}). Values are the mean ± s.d.mean of seven experiments and are expressed as OD (450 nm) per mg of protein of nuclear extract (**a**) and as OD (at 450 nm) per mg of protein (**b**). $^{\circ}P<0.001$ vs control; $^{*}P<0.05$, $^{**}P<0.005$ and $^{***}P<0.001$ vs CCl_4.

Materials

C4S from bovine trachea, CCl_4 and mineral oil were obtained from Sigma-Aldrich Srl (Milan, Italy). [^{14}C-]CCl_4 was provided by American Radiolabeled Chemicals Inc. (St Louis, MO, USA). Mouse MMP-2 and MMP-9 polyclonal antibodies were obtained from Chemicon International Inc., caspase-3 and caspase-7 monoclonal antibodies were purchased from Santa Cruz Biotecnology Inc. (Santa Cruz, CA, USA), cleaved caspase-3 and cleaved caspase-7 monoclonal antibodies were obtained from Cell Signaling Technology Inc. (Danvers, MA, USA), Horseradish peroxidase-labeled goat anti-rabbit antibodies were obtained from Imgenex Corporation (San Diego, CA, USA). All the other reagents used were purchased from Fluka (a division of Sigma-Aldrich Srl).

Results

Transaminase levels

Serum ALT and AST concentrations were evaluated to estimate the extent of hepatic damage. Table 1 reports the changes in activity of both transaminases in serum of mice at the end of the experiment. Low levels of ALT and AST activity were seen in the groups not treated with CCl_4, whereas a marked increase in the activity of the two enzymes was found in the serum of CCl_4-treated mice. The treatment of CCl_4 injected animals with C4S significantly reduced ALT and AST levels (Table 1). The reduction in transaminase release by hepatic cells was significant and dose-dependent.

NF-κB DNA-binding activity

Figure 1a shows the changes in NF-κB p50/65 heterodimer activation in the nuclear extract of hepatic cells. NF-κB DNA-binding activity was present at very low levels in the livers of untreated mice but NF-κB activation was markedly increased in CCl_4-treated mice. The acute treatment of animals with C4S resulted in a significant inhibition of NF-κB DNA binding, at all the doses of C4S used (Figure 1a).

Loss of IkBα protein in hepatic cell cytoplasm

Nuclear factor-κB activation was also investigated indirectly by studying its inhibitory protein, IkBα, in the hepatic cell cytoplasm (Figure 1b). Normal amounts of IkBα protein were assayed in CCl_4-untreated mice, whereas cirrhosis produced a significant reduction in IkBα protein in the cytoplasm of

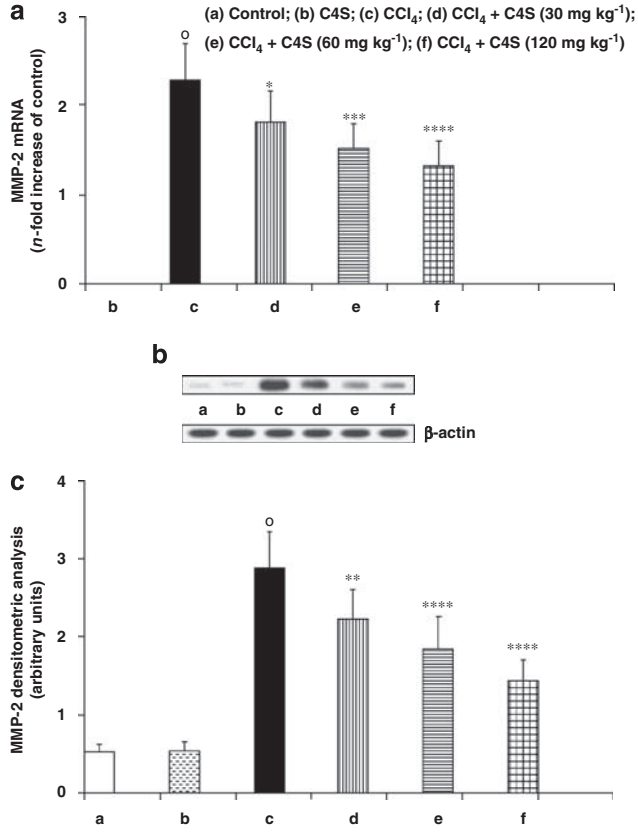

Figure 2 Effect of chondroitin-4-sulphate (C4S) treatment on hepatic metalloprotease (MMP)-2 mRNA expression (**a**) and related protein production (**b**, **c**) in livers of mice injected with carbon tetrachloride (CCl_4). Values are the mean ± s.d.mean of seven experiments and are expressed as *n*-fold increase with respect to the control (**a**) and as both densitometric analysis (**c**) and western blot analysis (**b**) for the MMP-2 protein levels. °$P<0.001$ vs control; *$P<0.05$, **$P<0.01$, ***$P<0.005$ and ****$P<0.001$ vs CCl_4.

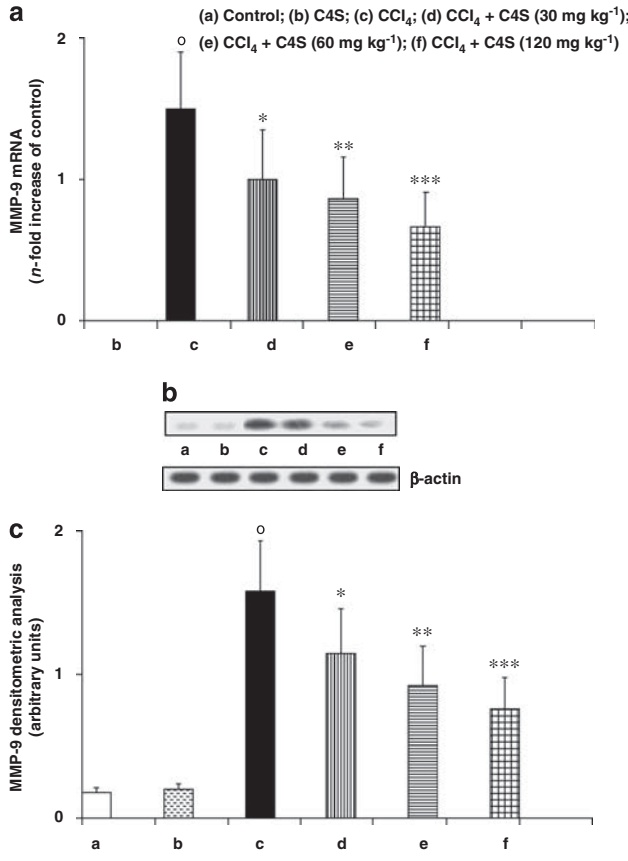

Figure 3 Effect of chondroitin-4-sulphate (C4S) treatment on hepatic metalloprotease (MMP)-9 mRNA expression (**a**) and MMP-9 protein production (**b**, **c**) in livers of mice injected with carbon tetrachloride (CCl_4). Values are the mean ± s.d.mean of seven experiments and are expressed as *n*-fold increase with respect to the control (**a**) and as both densitometric analysis (**c**) and western blot analysis (**b**) for the MMP-9 protein levels. °$P<0.001$ vs control; *$P<0.05$, **$P<0.005$ and ****$P<0.001$ vs CCl_4.

hepatic cells. The treatment of mice with C4S significantly blunted the phosphorylation of IkBα protein in the cytoplasm of hepatic cells.

MMP-2 and MMP-9 mRNA expression and protein activity

Metalloprotease-2 and MMP-9 were evaluated because of their active role in the destruction of liver ECM and its complex architecture (Figures 2a–c and 3a–c). Quantification of gene expression (Figures 2a and 3a) showed that the mRNA of these catalytic enzymes was not stimulated in control mice. However, MMP-2 and MMP-9 expression was significantly upregulated in the animals given CCl_4. The acute administration of C4S was able to reduce this increment in mRNA. The increase in MMP-2 and MMP-9 expression, in cirrhotic mice, correlated well with the increment in protein synthesis. This correlation also held for mice treated with C4S; the reduction in expression of mRNA for MMP-2 and MMP-9 corresponded with a similar diminution in protein formation (Figures 2b, c, 3b and c).

Caspase-3 and caspase-7 mRNA expression and protein activity

The apoptotic activators caspase-3 and caspase-7 were evaluated by measuring caspase-3 and caspase-7 mRNA expression and procaspase-3, cleaved caspase-3, procaspase-7 and cleaved caspase-7 protein activity to estimate apoptosis in liver tissue. Caspase-3 (Figure 4a) and caspase-7 (Figure 5a) mRNA evaluation and protein activity (Figures 4b, c, 5b and c) in mice with CCl_4-induced hepatitis showed a marked increase in the expression of the two apoptotic proteases. The treatment of animals with C4S was able to prevent

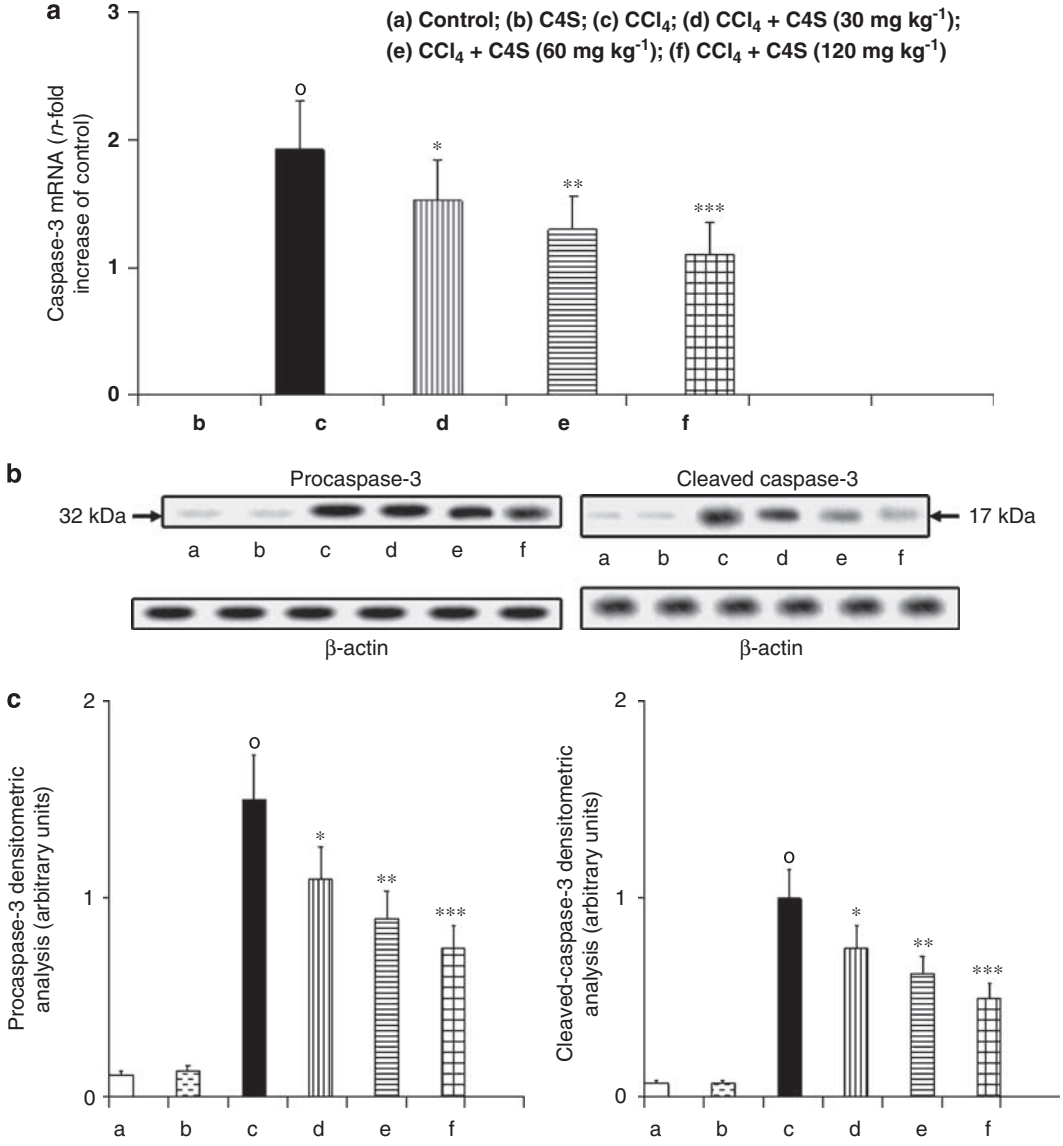

Figure 4 Effect of chondroitin-4-sulphate (C4S) treatment on hepatic caspase-3 mRNA expression (**a**) and related protein production procaspase-3 and cleaved caspase-3 (**b**, **c**) in livers of mice injected with carbon tetrachloride (CCl_4). Values are the mean ± s.d.mean of seven experiments and are expressed as *n*-fold increase with respect to the control (**a**) and as both densitometric analysis (**c**) and western blot analysis (**b**) for the procaspase-3 and cleaved caspase-3 protein levels. °$P<0.001$ vs control; *$P<0.05$, **$P<0.005$ and ***$P<0.001$ vs CCl_4.

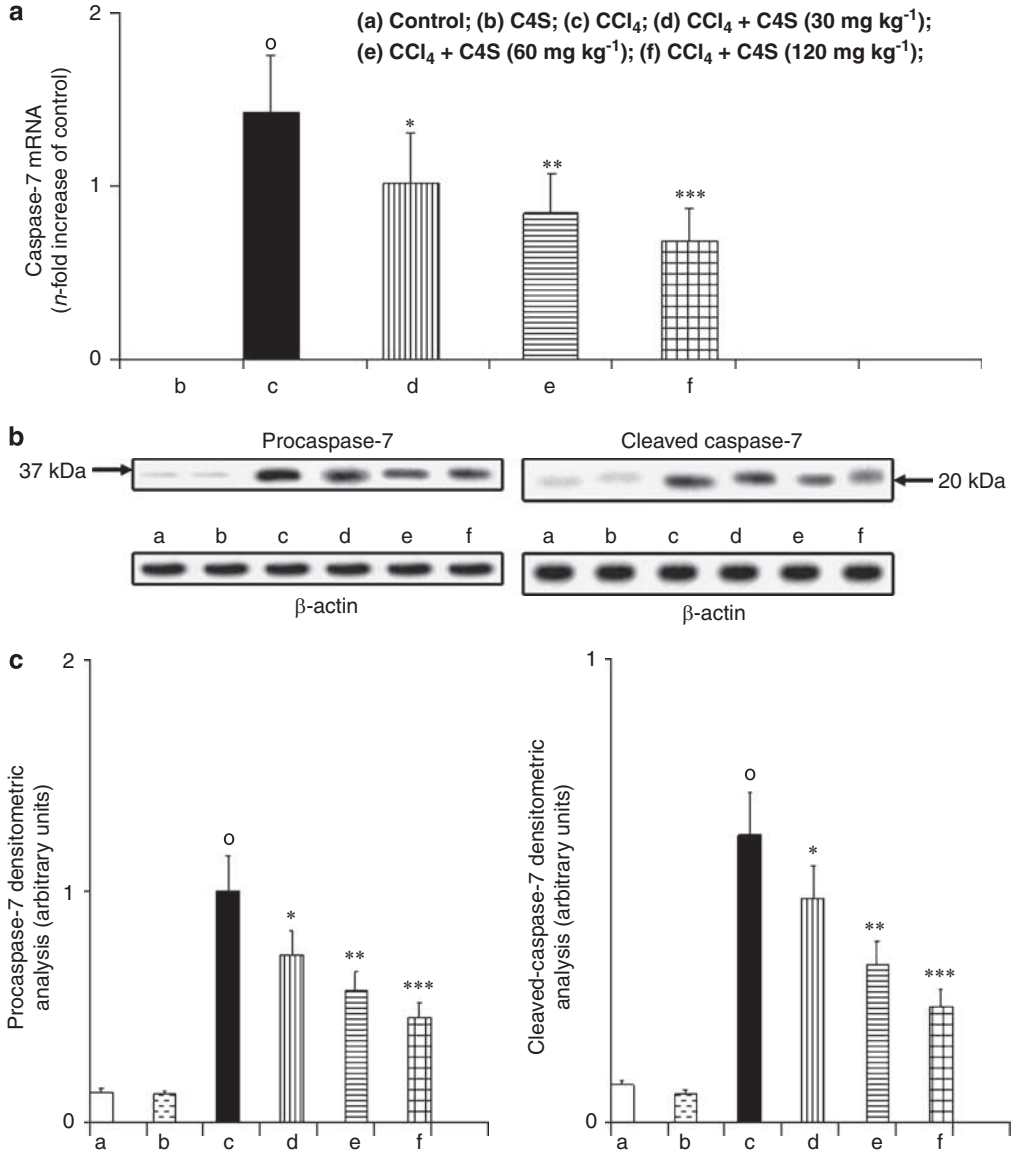

Figure 5 Effect of chondroitin-4-sulphate (C4S) treatment on hepatic caspase-7 mRNA expression (**a**) and related protein production procaspase-7 and cleaved caspase-7 (**b**, **c**) in livers of mice injected with carbon tetrachloride (CCl_4). Values are the mean ± s.d.mean of seven experiments and are expressed as *n*-fold increase with respect to the control (**a**) and as both densitometric analysis (**c**) and western blot analysis (**b**) for the procaspase-7 and cleaved caspase-3 protein levels. °$P<0.001$ vs control; *$P<0.05$, **$P<0.005$ and ***$P<0.001$ vs CCl_4.

caspase-3 and caspase-7 mRNA expression and new protein generation. Once again, caspase-3 and caspase-7 mRNA levels correlated well with the protein concentration obtained by western blot analysis, and the amount of active caspase-3 and caspase-7 correlated well with the zymogens procaspase-3 and procaspase-7, respectively (Figures 4b, c, 5b and c).

8-IPE evaluation

Determination of 8-IPE in liver tissue was carried out to estimate the lipid peroxidation of hepatic membranes (Table 2). The low levels of 8-IPE were measured in untreated mice, whereas a significant increment in this marker was found in the hepatic cells of mice treated with CCl_4. Acute treatment with C4S reduced 8-IPE levels probably by inhibiting membrane lipid peroxidation consequent on chelation of transition metals.

ELA levels

Neutrophil infiltration to the damaged tissue contributes to the progression and the spread of inflammation (Table 2). Very low ELA concentrations were measured in untreated mice. In contrast, elevated ELA levels were assayed in the

Table 2 Effect of C4S treatment on 8-isoprostane content and elastase levels in hepatic tissue of mice after CCl_4 injection

Experimental group	*8-isoprostane*	*Elastase*
Control	2.3 ± 0.4	0.34 ± 0.05
C4S (120 mg kg^{-1})	2.1 ± 0.4	0.29 ± 0.04
CCl_4	57.3 ± 8.2†	2.34 ± 0.45†
CCl_4 + C4S (30 mg kg^{-1})	32.4 ± 6.1**	1.50 ± 0.35*
CCl_4 + C4S (60 mg kg^{-1})	23.5 ± 5.2**	1.28 ± 0.34**
CCl_4 + C4S (120 mg kg^{-1})	17.2 ± 4.0**	1.09 ± 0.31**

Abbreviations: ALT, alanine aminotransferase; AST, aspartate aminotransferase; CCl_4, carbon tetrachloride; C4S, chondroitin-4-sulphate.
Values are the mean ± s.d.mean of seven experiments and are expressed as pg mg^{-1} of protein for 8-isoprostane and as fluorescent arbitrary U mg^{-1} of protein for elastase.
$^{\dagger}P<0.001$ vs control; $^{*}P<0.005$ and $^{**}P<0.001$ vs CCl_4.

Table 3 Effect of C4S treatment on SOD activity and GSH levels in hepatic tissue of mice after CCl_4 injection

Experimental group	*SOD*	*GSH*
Control	14.4 ± 3.2	17.9 ± 4.1
C4S (120 mg kg^{-1})	13.8 ± 3.6	18.3 ± 4.3
CCl_4	4.0 ± 1.4†	5.4 ± 1.8†
CCl_4 + C4S (30 mg kg^{-1})	7.6 ± 1.7*	9.8 ± 2.1*
CCl_4 + C4S (60 mg kg^{-1})	9.8 ± 2.0*	12.5 ± 2.3*
CCl_4 + C4S (120 mg kg^{-1})	12.3 ± 2.7*	15.1 ± 2.7*

Abbreviations: ALT, alanine aminotransferase; AST, aspartate aminotransferase; CCl_4, carbon tetrachloride; C4S, chondroitin-4-sulphate; GSH, reduced glutathione; SOD, superoxide dismutase.
Values are the mean ± s.d.mean of seven experiments and are expressed as U mg^{-1} of protein for SOD and as nmol mg^{-1} of protein for GSH.
$^{\dagger}P<0.001$ vs control; $^{*}P<0.001$ vs CCl_4.

group given CCl_4 alone. The administration of C4S had a beneficial effect by reducing PMN accumulation in the liver, as demonstrated by the decreased ELA levels.

Endogenous antioxidants

The concentrations of SOD and total GSH (Table 3) were assayed to evaluate the integrity of the antioxidant balance downregulated by hepatitis. A significant reduction in both antioxidants was observed in the liver tissue obtained from mice given CCl_4. Once again, the treatment with C4S significantly restored both SOD and GSH activity. Additional groups of mice were also treated with $CCl4^{+}$/-C4S with the aim to investigate any possible effect of C4S on rate of GSH resynthesis. Figure 8 shows the GSH values obtained at multiple time points. As shown, C4S by itself had no effect in hepatic GSH content since values were unchanged, every 4 h throughout the experiment. Also in mice treated with CCl_4 plus C4S, GSH concentrations were almost similar, thus demonstrating that C4S had no effect on the rate of GSH resynthesis.

Histology

Figure 6 shows the histological changes occurring at the end of the experiment. Figures 6a and b show a liver section from an untreated mouse. The cells appear complete, without any infiltrations or haemorrhagic signs. shows a liver section from a CCl_4-treated mouse. Centrilobular haemorrhagic alterations, broad infiltration of lymphocytes,

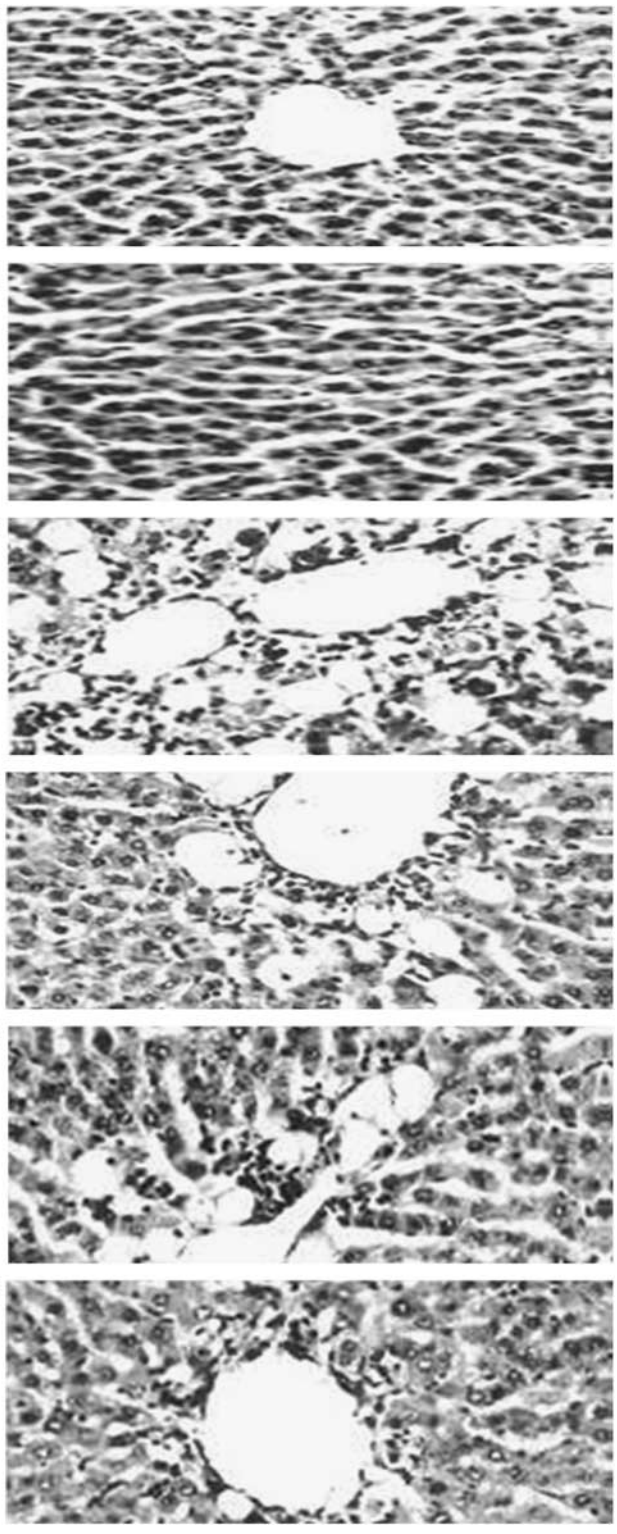

Figure 6 Effect of chondroitin-4-sulphate (C4S) on histological analysis of hepatic tissue, after injection with carbon tetrachloride (CCl_4). (**a**) Control; (**b**) C4S (120 mg kg^{-1}); (**c**) CCl_4; (**d**) CCl_4 + C4S (30 mg kg^{-1}); (**e**) CCl_4 + C4S (60 mg kg^{-1}); (**f**) CCl_4 + C4S (120 mg kg^{-1}). Haematoxylin–eosin × 1800.

loss of cellular boundary, hydropic degeneration and fatty change are evident. The necrosis is massive, involving whole groups of lobules in their entirety. In Figures 6d, e and f a representative selection of livers from mice receiving CCl_4 and C4S treatment show that a gradual reduction occurred in hepatocellular lesions, fatty change and alterations (Figure 6).

Covalent binding

$[^{14}C]CCl_4$-derived covalently bound radiolabel to liver macromolecules is a reliable measure of the extent of CCl_4 bioactivation. As reported in Figure 7, the amount of label covalently bound to liver proteins was not different among the group treated with $[^{14}C]CCl_4$ alone compared with groups treated with $[^{14}C]CCl_4$ plus C4S. These results demonstrated that the protective effect exerted by C4S in CCl_4-induced hepatic toxicity was independent of CCl_4 bioactivation.

Discussion

In this study, the treatment of acute hepatis in mice using different doses of C4S was able to prevent cell damage induced by CCl_4 treatment. Results concurred with our previous experiments, albeit using two different types of animals (Campo *et al*., 2004a, b). In addition to the antioxidant effect of this glycosaminoglycan, the focus of this study was C4S activity on NF-κB and the modulation of apoptosis. We previously reported that synergistic treatment, of stressed skin fibroblasts, with hyaluronic acid and C4S, reduced NF-κB and activation of caspases (Campo *et al*., 2008). We concluded that this reduction was a consequence of ROS inhibition. As our results demonstrated that C4S affected neither CCl_4 bioactivation nor the rate of GSH resynthesis, it was plausible to hypothesize, also in this *in vivo* model, that the inhibition of NF-κB DNA binding to the nucleus is probably the consequence of C4S decreasing ROS production in liver tissue. NF-κB activation requires sequential phosphorylation and degradation of IkBα, which finally disappears from the cytoplasm. As ROS are able to activate this pathway, then C4S also prevents the loss of the inhibitory protein from the cytoplasm by preventing the oxidative burst. Although several papers have reported that CS may also directly inhibit NF-κB activation and apoptosis (Cartel and Post, 2005; Rolls *et al*., 2006), we suggest that the same proposal for NF-κB DNA binding exerted by ROS may be extended to activation of the apoptotic process. However, a direct involvement of C4S cannot be excluded. Iron is a mediator of CCl_4 hepatoxicity, and it may be sequestered by chelation. Therefore, attention should be focused on the fact that C4S reduced damage by not only decreasing ROS generation in hepatic tissue, but also by inhibiting executioner caspases and MMPs activation, in turn, activated by NF-κB translocation.

Caspases, translated as zymogens, are processed proteolytically to become mature active enzymes. There are two broad categories of caspases: the initiator caspases activated through upstream events, which in turn, activate the downstream effector or executioner caspases. The three executioner caspases cleave a subset of intracellular proteins to promote the characteristic apoptotic morphology. There are two major pathways through which apoptosis is induced; one involves death receptors and is exemplified by

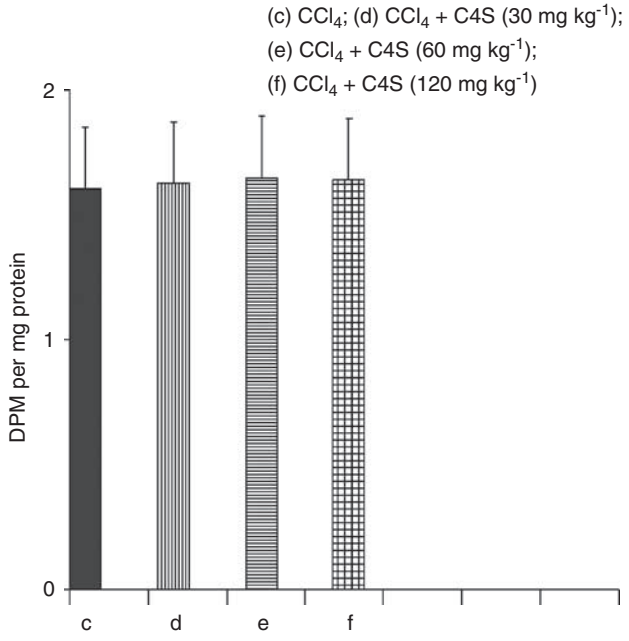

Figure 7 Covalent binding of $[^{14}C]CCl_4$-derived radiolabel to liver tissue, evaluated in mice treated with carbon tetrachloride (CCl_4) alone and CCl_4 plus chondroitin-4-sulphate (C4S). Values are the mean ± s.d.mean of seven experiments and are expressed as disintegrations per minute per mg of protein.

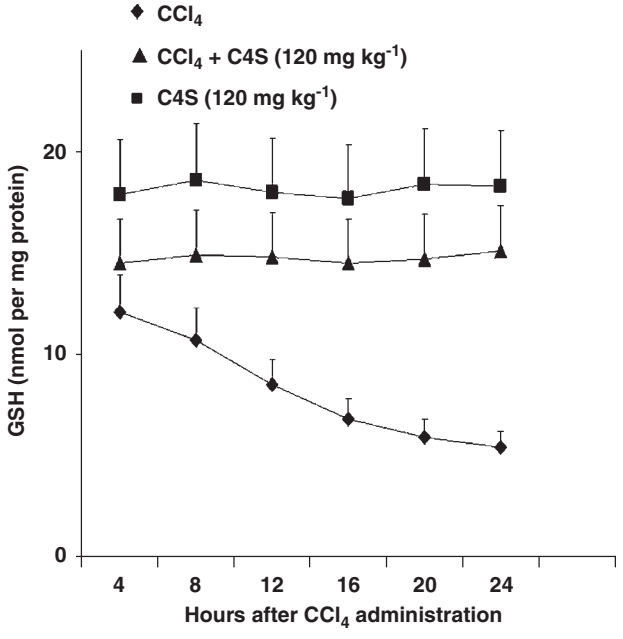

Figure 8 Reduced glutathione (GSH) content of liver tissue assessed at several time points in mice treated with carbon tetrachloride (CCl_4) alone, chondroitin-4-sulphate (C4S) alone and CCl_4 plus C4S. Values are the mean ± s.d.mean of seven experiments and are expressed as nmol mg^{-1} of protein.

Fas-mediated caspase-8 activation, and the other is the stress- or mitochondria-mediated caspase-9 activation pathway. Both pathways converge on caspase-3 and caspase-7 activation, resulting in nuclear degradation and cellular morphological changes. Oxidative stress induces cytochrome *c* release from mitochondria and activation of caspases, p53 and kinases (Oral *et al*., 2006). It has been reported that molecules capable of scavenging ROS may reduce apoptosis activation and cell disruption (Ham *et al*., 2006). In our experiments, the restricted ROS production was able to reduce the executioner caspase-3 and caspase-7 activation pathway, with the consequent decrease of apoptotic changes.

Metalloproteases are involved in a number of physiological and pathological processes such as tissue remodelling, morphogenesis, wound healing and inflammation (Clark *et al*., 2008). Several MMPs are upregulated in inflammation and among them MMP-2 and MMP-9 are deeply involved in the degradation of the ECM components. ROS are a potent stimulus for the upregulation of MMPs (Poli, 2000), and this was further supported by the finding that antioxidants limit the imbalance of MMPs (Nelson and Melendez, 2004). In our study, the treatment of CCl_4-intoxicated mice with C4S was able to decrease MMP-2 and MMP-9 upregulation with a consequent limitation in liver damage. In addition, it is widely known that oxidative stress produces a series of reactive intermediates, such as H_2O_2, $O_2^-\cdot$, OH·, lipid peroxides, NO· and so on, that may damage the cell directly through their chemical action or may indirectly produce injury by activating a multitude of other different mechanisms, including NF-κB and caspase activation. Both these mechanisms are able to disrupt the cell through the activation of inflammatory processes or through apoptosis. Total oxidative damage is therefore because of both direct and indirect mechanisms. Previously published data suggest that ROS are involved in NF-κB and apoptosis activation during inflammation and particularly in liver diseases (Lee *et al*., 1997; Orfila *et al*., 2005; Pantano *et al*., 2006). Antioxidants that, for instance, prevent lipid peroxidation by decreasing the detrimental actions of the OH· radical, do not have any effect on H_2O_2 or $O_2^-\cdot$ production. Direct damage on cellular membranes is thereby prevented. However, NF-κB and caspase activation may be induced by H_2O_2 or O_2^-. In such cases, these selective antioxidants have no effect on NF-κB and apoptosis induction during the oxidative process. The same concept may be extended to antioxidants that, for instance, scavenge only H_2O_2 or other specific ROS. It has been hypothesized that the antioxidant effect of C4S is exerted by chelating transition metal ions. As the Haber–Weiss and Fenton reactions are primed by transition metal ions such as Fe^{++}, and the effect of the chelation of this metal ion reduces oxidative stress by eliminating the product of this reaction, it is reasonable to hypothesize that it is more efficient to act by blocking this reaction than by scavenging the products formed. In this way, C4S activity would be more efficient than a conventional antioxidant, because the inhibition of the oxidative burst does not prime NF-κB and apoptosis. However, this evidence has yet to be fully confirmed, as other studies have reported that the antioxidant activity of C4S derives from the direct neutralization of ROS because of its chemical interaction, mainly with OH· radicals (Arai *et al*., 1999; Maksimenko, 2005). If this were so, the antioxidant effect of C4S would be independent from NF-κB and caspase activation. Instead, the treatment of mice with C4S was able to protect hepatic cells from oxidative injury and also to inhibit NF-κB DNA binding and apoptosis by two separate mechanisms. This study is a further confirmation that the antioxidant effect of C4S is because of the blocking of Haber–Weiss and Fenton's reactions by metal ion chelation. Nevertheless, that C4S may exert a direct effect on NF-κB and apoptosis inhibition cannot be excluded.

Acknowledgements

This study was supported by a grant PRA (Research Athenaeum Project 2004) from the University of Messina, Italy.

Conflict of interest

The authors state no conflict of interest.

References

Arai H, Kashiwagi S, Nagasaka Y, Uchida K, Hoshii Y, Nakamura K (1999). Oxidative modification of apolipoprotein E in human very-low-density lipoprotein and its inhibition by glycosaminoglycans. *Arch Biochem Biophys* **367**: 1–8.

Bhattacharyya J, Biswas S, Datta AG (2004). Mode of action of endotoxin: role of free radicals and antioxidants. *Curr Med Chem* **11**: 359–368.

Blair PC, Thompson MB, Wilson RE, Esber HH, Maronpot RR (1991). Correlation of changes in serum analytes and hepatic histopathology in rats exposed to carbon tetrachloride. *Toxicol Lett* **55**: 149–159.

Bradford MM (1976). A rapid and sensitive method for the quantitation of microgram quantities of protein utilizing the principle of protein-dye binding. *Anal Biochem* **72**: 248–254.

Bustin SA (2000). Absolute quantification of mRNA using real-time reverse transcription polymerase chain reaction assays. *J Mol Endocrinol* **25**: 169–193.

Campo GM, Avenoso A, Campo S, D'Ascola A, Ferlazzo AM, Calatroni A (2004a). The antioxidant and antifibrogenic effect of the glycosaminoglycans hyaluronic acid and chondroitin-4-sulphate in a subchronic rat model of carbon tetrachloride-induced liver fibrogenesis. *Chem Biol Interact* **148**: 125–138.

Campo GM, Avenoso A, Campo S, D'Ascola A, Traina P, Samà D *et al*. (2008). NF-kB and caspases are involved in the hyaluronan and chondroitin-4-sulphate exerted antioxidant effect in fibroblast cultures exposed to oxidative stress. *J Appl Toxicol* **28**: 309–317.

Campo GM, Avenoso A, Campo S, Ferlazzo AM, Calatroni A (2006). Chondroitin sulphate: antioxidant properties and beneficial effects. *Mini Rev Med Chem* **6**: 1311–1320.

Campo GM, Avenoso A, Campo S, Ferlazzo AM, Micali C, Zangh L *et al*. (2004b). Hyaluronic acid and chondroitin-4-sulphate treatment reduces damage in carbon tetrachloride-induced acute rat liver injury. *Life Sciences* **74**: 1289–1305.

Campo GM, D'Ascola A, Avenoso A, Campo S, Ferlazzo AM, Micali C *et al*. (2004c). Glycosaminoglycans reduce oxidative damage induced by copper (Cu + 2), iron (Fe + 2) and hydrogen peroxide (H2O2) in human fibroblast cultures. *Glycoconj J* **20**: 133–141.

Cartel NJ, Post M (2005). Abrogation of apoptosis through PDGF-BB-induced sulphated glycosaminoglycans synthesis and secretion. *Am J Physiol Lung Cell Mol Physiol* **288**: L285–L293.

Clark IM, Swingler TE, Sampieri CL, Edwards DR (2008). The regulation of matrix metalloproteinases and their inhibitors. *Int J Biochem Cell Biol* **40**: 1362–1378.

Ding WX, Yin XM (2004). Dissection of the multiple mechanisms of TNF-α-induced apoptosis in liver injury. *J Cell Mol Med* **8**: 445–454.

Genestra M (2007). Oxyl radicals, redox-sensitive signalling cascades and antioxidants. *Cell Signal* **19**: 1807–1819.

Ham YM, Lim JH, Na HK, Choi JS, Park BD, Yim H *et al*. (2006). Ginsenoside-Rh2-induced mitochondrial depolarization and apoptosis are associated with ROS-and Ca2+-mediated JNK1 activation in HeLa cells. *J Pharmacol Exp Ther* **319**: 1276–1285.

Heyninck K, Wullaert A, Beyaert R (2003). Nuclear factor-kappa B plays a central role in tumor necrosis factor-mediated liver disease. *Biochem Pharmacol* **66**: 1409–1415.

Kundu JK, Shin YK, Surh YJ (2006). Resveratrol modulates phorbol ester-induced pro-inflammatory signal transduction pathways in mouse skin *in vivo*: NF-kappaB and AP-1 as prime targets. *Biochem Pharmacol* **72**: 1506–1515.

Lee KS, Cottam HB, Houglum K, Wasson DB, Carson D, Chojkier M (1997). Pentoxifylline blocks hepatic stellate cell activation independently of phosphodiesterase inhibitory activity. *Am J Physiol* **273**: G1094–G1100.

Maksimenko AV (2005). Experimental antioxidant biotherapy for protection of the vascular wall by modified forms of superoxide dismutase and catalase. *Curr Pharm Des* **11**: 2007–2016.

Malhi H, Gores GJ, Lemasters JJ (2006). Apoptosis and necrosis in the liver: a tale of two deaths? *Hepatology* **43**: S31–S44.

Nelson KK, Melendez JA (2004). Mitochondrial redox control of matrix metalloproteinases. *Free Radic Biol Med* **37**: 768–784.

Oral B, Guney M, Demirin H, Ozguner M, Giray SG, Take G *et al*. (2006). Endometrial damage and apoptosis in rats induced by dichlorvos and ameliorating effect of antioxidant Vitamins E and C. *Reprod Toxicol* **22**: 783–790.

Orfila C, Lepert JC, Alric L, Carrera G, Beraud M, Pipy B (2005). Immunohistochemical distribution of activated nuclear factor kappaB and peroxisome proliferators-activated receptors in carbon tetrachloride-induced chronic liver injury in rats. *Histochem Cell Biol* **123**: 585–593.

Ozben T (2007). Oxidative stress and apoptosis: impact on cancer therapy. *J Pharm Sci* **96**: 2181–2196.

Pantano C, Reynaert NL, van der Vliet A, Janssen-Heininger YM (2006). Redox-sensitive kinases of the nuclear factor-kappaB signaling pathway. *Antioxid Redox Signal* **8**: 1791–1806.

Pineiro-Carrero VM, Pineiro EO (2004). Liver. *Pediatrics* **113**: 1097–1106.

Poli G (2000). Pathogenesis of liver fibrosis: role of oxidative stress. *Mol Aspects Med* **21**: 49–98.

Rolls A, Cahalon L, Bakalash S, Avidan H, Lider O, Schwartz M (2006). Asulphated disaccharide derived from chondroitin sulphate proteoglycan protects against inflammation-associated neurodegeneration. *FASEB J* **20**: 547–549.

Sawant SP, Dnyanmote AV, Shankar K, Limaye PB, Latendresse JR, Mehendale HM (2004). Potentiation of carbon tetrachloride hepatotoxicity and lethality in type 2 diabetic rats. *J Pharmacol Exp Ther* **308**: 694–704.

Schattenberg JM, Galle PR, Schuchmann M (2006). Apoptosis in liver disease. *Liver Int* **26**: 904–911.

Stehbens WE (2003). Oxidative stress, toxic hepatitis, and antioxidants with particular emphasis on zinc. *Exp Mol Pathol* **75**: 265–276.

Sun AY, Ingelman-Sunberg M, Neve E, Matsumoto H, Nishitani Y, Minowa Y *et al*. (2001). Ethanol and oxidative stress. *Alcohol Clin Exp Res* **25** (5 Suppl ISBRA): 237S–243S.

Volpi N (2006). Chondroitin sulfate: structure, role and pharmacological activity. *Adv Pharmacol Elsevier* **53**.

Wang T, Shankar K, Ronis MJ, Mehendale HM (2007). Mechanisms and outcomes of drug- and toxicant-induced liver toxicity in diabetes. *Crit Rev Toxicol* **37**: 413–459.

Waris G, Tardif KD, Siddiqui A (2002). Endoplasmic reticulum (ER) stress: hepatitis C virus induces an ER-nucleus signal transduction pathway and activates NF-kappaB and STAT-3. *Biochem Pharmacol* **64**: 1425–1430.

Weber LW, Boll M, Stampfl A (2003). Hepatotoxicity and mechanism of action of haloakanes: carbon tetrachloride as a toxicological model. *Crit Rev Toxicol* **33**: 105–136.

Weiler-Normann C, Herkel J, Lohse AW (2007). Mouse models of liver fibrosis. *Z Gastroenterol* **45**: 43–50.

Wu D, Zhai Q, Shi X (2006). Alcohol-induced oxidative stress and cell responses. *J Gastroenterol Hepatol* **21** (Suppl.3): S26–S29.